Optik 128 (2017) 26–33

Contents lists available at ScienceDirect

Optik

journal homepage: www.elsevier.de/ijleo

Original research article

Study on molten salt synthesis, microstructural determination and white light emitting properties of $CoNb_2O_6$:Dy^{3+} phosphor

Mete Kaan Ekmekçi[a,*], Mustafa İlhan[b], Lütfiye Feray Güleryüz[c], Ayhan Mergen[b]

[a] Marmara University, Department of Chemistry, Kadıkoy, 34777, Istanbul, Turkey
[b] Marmara University, Deparment of Material and Metalurgy Eng., Kadıkoy, 34777, Istanbul, Turkey
[c] Ege University, Graduate School of Natural and Applied Science, Bornova, 35040, Izmir, Turkey

ARTICLE INFO

Article history:
Received 3 August 2016
Accepted 3 October 2016

Keywords:
Cobalt niobate
XRD
SEM-EDS
Optical properties
White LEDs

ABSTRACT

Undoped, 0.5, 3 and 6 mol% Dy^{3+} doped $CoNb_2O_6$ powders have been prepared by molten salt method using cobalt nitrate hexa hydrate, niobium oxide, dysprosium oxide and Li_2SO_4—Na_2SO_4 salt mixture as a flux at 800 °C for 4 h. X-ray diffraction patterns of the undoped, 0.5 and 3 mol% doped $CoNb_2O_6$ samples exhibited a single orthorhombic columbite phase, while 6 mol% Dy^{3+} doped powder showed minor phase. SEM-EDS results coonfirmed XRD findings and revealed smaller grain size by increasing Dy^{3+} concentration. Structural and luminescence properties of Dy^{3+} doped samples in UV–vis spectral region were studied. The emissions increased with increasing doping concentration up to 3 mol%, and then decreased due to concentration quenching effect. The color chromaticity temperature (CCT) data of all samples have been estimated in white light region and color of light appear close to yellowish-green.

© 2016 Elsevier GmbH. All rights reserved.

1. Introduction

The demands of newer technologies in many different fields such as lighting, medical, military, laser applications, high energy photoluminescent (plasma panels) and cathodoluminescent flat panel displays, holography and entertainment industry have produced a search for new functional materials and synthesis routes to improve the performance of phosphors. Rare-earth activated oxide phosphors exhibit luminescence arising from the 3d → 3d, 5d → 4f or 4f → 4f transitions. The performance of optical materials require high purity, single phase and reduced particle size with uniform composition for the new flat panel display developments [1–3]. Moreover, in recent years, white light emitting diodes (W-LEDs) have been considered as next generation solid state lighting sources due to the advantages of long lifetime, energy saving, high efficiency, reliability and environmentally friendly properties [4]. Trivalent dysprosium (Dy^{3+}) ion has two typical energy bands in the 4f-4f emission spectrum, namely, the yellow band around 570–590 nm due to $^4F_{9/2} \rightarrow {}^6H_{13/2}$ transition and the blue band about 475–495 nm due to $^4F_{9/2} \rightarrow {}^6H_{15/2}$ transition. In addition, suitable yellow to blue (Y/B) emission intensity ratio possess a white light generation for Dy^{3+} doped phosphor materials. Besides, the intensity ratio of the two emission bands are depend on the host crystal structure [5,6].

* Corresponding author.
E-mail address: mekmekci@marmara.edu.tr (M.K. Ekmekçi).

http://dx.doi.org/10.1016/j.ijleo.2016.10.012
0030-4026/© 2016 Elsevier GmbH. All rights reserved.

The columbite-type niobates having AB_2O_6 (A = Ba^{2+},Sr^{2+},Mg^{2+},Sn^{2+},Zn^{2+}, etc. B = Nb^{5+}) general formula offers many advantages with their optical, magnetic and dielectric properties and they may be relevant for the above mentioned demands [7–9]. Among the columbite niobates, $CoNb_2O_6$ crystallizes in both columbite (orthorhombic) and trirutil (tetragonal) structures. The orthorhombic columbite structure consists of MO_6 octahedras (M = Co or Nb) by sharing edges and forming chains along the c-axis. In this structure, parallel CoO_6 and NbO_6 chains alternate along the b-axis [10,11]. $CoNb_2O_6$ is a good candidate being as a coating material for mechanical filters such as for resonators and capacitors [12,13]. $CoNb_2O_6$ exhibits the quasi-one-dimensional Ising magnetic properties at 2.95 K [14]. The gas sensing behavior of $CoNb_2O_6$ was investgated by Balamurugan et al. [15]. $CoNb_2O_6$ is well known compound for the preparation of single phase perovskite $Pb(Co_{1/3}Nb_{2/3})O_3$, which have importance for multilayer ceramic capacitor, transducer, electrostrictor and actuator applications [16,17]. $CoNb_2O_6$ was also reported to be a potential microwave dielectric resonator material [18–20].

Several different synthesis techniques have been used to prepare $CoNb_2O_6$, such as solid state synthesis [21], co-precipitation [22] and hydrothermal [23] methods. On the other hand, molten salt route provides lower calcination temperature and heat treatment time than that of the conventional solid state method to prepare $CoNb_2O_6$. Besides, molten salt synthesis helps to provide high homogenity, single phase formation, and a small particle size in one-step reaction [24,25].

Although a few studies have been ascribed, no enough work has been reported about the luminescence properties of $CoNb_2O_6$ phosphors in the literature. Therefore, in this study, structural and luminescence properties of undoped and Dy^{3+} doped columbite $CoNb_2O_6$ phosphors have been investigated by using XRD, SEM-EDS and Photoluminescence analyses.

2. Experimental

Undoped and 0.5, 3 and 6 mol% Dy^{3+} doped $CoNb_2O_6$ columbite ceramic powders were synthesized via molten salt route by mixing starting materials of cobalt nitrate [$Co(NO_3)_2{\cdot}6H_2O$] and niobium oxide (Nb_2O_5) at a salt to oxide weight ratio of 2:1. Li_2SO_4—Na_2SO_4 salt mixture was used at molar ratio of 0.635/0.365. After mixing of starting materials (cobalt nitrate, niobium oxide, and dysprosium oxide) in an agate mortar, Li_2SO_4 and Na_2SO_4 salt mixture was subsequently added and ground together with the first mixture. Then they were mixed well to provide homogeneity. After calcining of sufficient amount of mixture at 800 °C for 4 h in an alumina crucible, they were washed with ultrapure water and vacuum filtered several times in order to remove ionic salts from the oxides. The presence of the sulfate ions in filtrate were controlled by qualitative reactions. The surface morphology, microstructure and phase detection of powders were performed by scanning electron microscopy (SEM; Jeol JSM 5910LV) equipped with energy dispersive spectroscopy (EDS; Oxford Instruments Inca X-Sight 7274). The phase determination in sintered samples were investigated by X-ray diffractometer (XRD, Rigaku Corp., D-MAX 2200) using Cu-K_α radiation at a scan rate of 2°/min between 20 and 65° and Ni filter. Photoluminescence (PL) measurements, excitation and emission spectra were recorded by using a Scinco floromaster-FS/2 model fluorometer with a Xe-arc lamp (150 W) as excitation source. All of the measurements were carried out at room temperature.

3. Results and discussion

3.1. X-ray diffraction and SEM-EDS analyses

Fig. 1 shows the XRD results of undoped and Dy^{3+} doped $CoNb_2O_6$ samples synthesized by using the Li_2SO_4/Na_2SO_4 salt system and 2:1 salt to oxide molar ratio with calcination time of 4 h at 800 °C. Both undoped and Dy^{3+} doped $CoNb_2O_6$ phases crystallized (JCPDS card no: 32-0304) in orthorhombic symmetry with space group *Pbcn*(60) having the columbite type structure. Single phase has been determined for undoped, 0.5 and 3 mol% Dy^{3+} doping concentrations, while $DyNbO_4$ (JCPDS card no: 22-1099) minor phase has occurred for 6 mol% Dy^{3+} doping concentration.

As seen from Fig. 2, there are three kinds of empty octahedral sites as *4a*, *4b* and *8d* in the columbite structure [26] in which the ion's radius and CN (coordination number) of Co^{+2} (CoO_6) and Nb^{+5} (NbO_6) are 0.65 Å (for 6 C.N) and 0.64 Å (for 6 C.N) respectively. Among the octahedral (*4a,4b,8d*) sites, when Dy^{3+} ions insert into *8d* sites, this may lead to a large repulsive force on adjacent Nb^{5+} ions. On the other hand, the *4b* sites are compressed due to the Jahn-Teller distortion of adjacent CoO_6 octahedral, while the *4a* sites are relatively free. The *4b* sites deformation would become relaxed if the Jahn-Teller Co^{2+} cations disappear. Hence, based on the ion's radius and valence, the Dy^{3+} ions having an ionic radius of 0.912 Å (for 6 C.N) might occupy firstly *4a* and then *4b* sites up to 3 mol% doped concentration [26]. Also, Fig. 3 shows a shift to higher 2 theta angles for (311) peak depending on the Dy^{3+} concentrations. As expected, a decrease in lattice constant may be attributed to shrinkage of the lattice. These peak shifts revealed the presence of strains in the doped host lattices. This situation indicated the successful location of Dy^{3+} ions in the lattice up to 6 mol%. Also, the incorporation of Dy^{3+} ions has caused a change in the phase structure of $CoNb_2O_6$ above 3 mol% concentration. Accordingly, while Dy^{3+} ions occupied mostly the *4a*, and *4b* sites, a small amount of Dy^{3+} ions might have distorted the NbO_6 octahedral and promoted the formation of $DyNbO_4$ minor phase.

Fig. 4(a–d) shows the SEM micrographs of undoped, 0.5, 3 and 6 mol% Dy^{3+} doped samples at 10.000× magnification. SEM analysis revealed that the grain size of $CoNb_2O_6$ decreased for doped samples with the increasing concentrations of Dy^{3+} ions. The structures of Dy^{3+} doped $CoNb_2O_6$ powders exhibited oval like shapes and submicron grain sizes varied between 0.2 and 0.8 μm. SEM-EDS micrographs of 6 mol% Dy^{3+} doped sample was given at low (5.000×) and high (10.000×) magnifications in

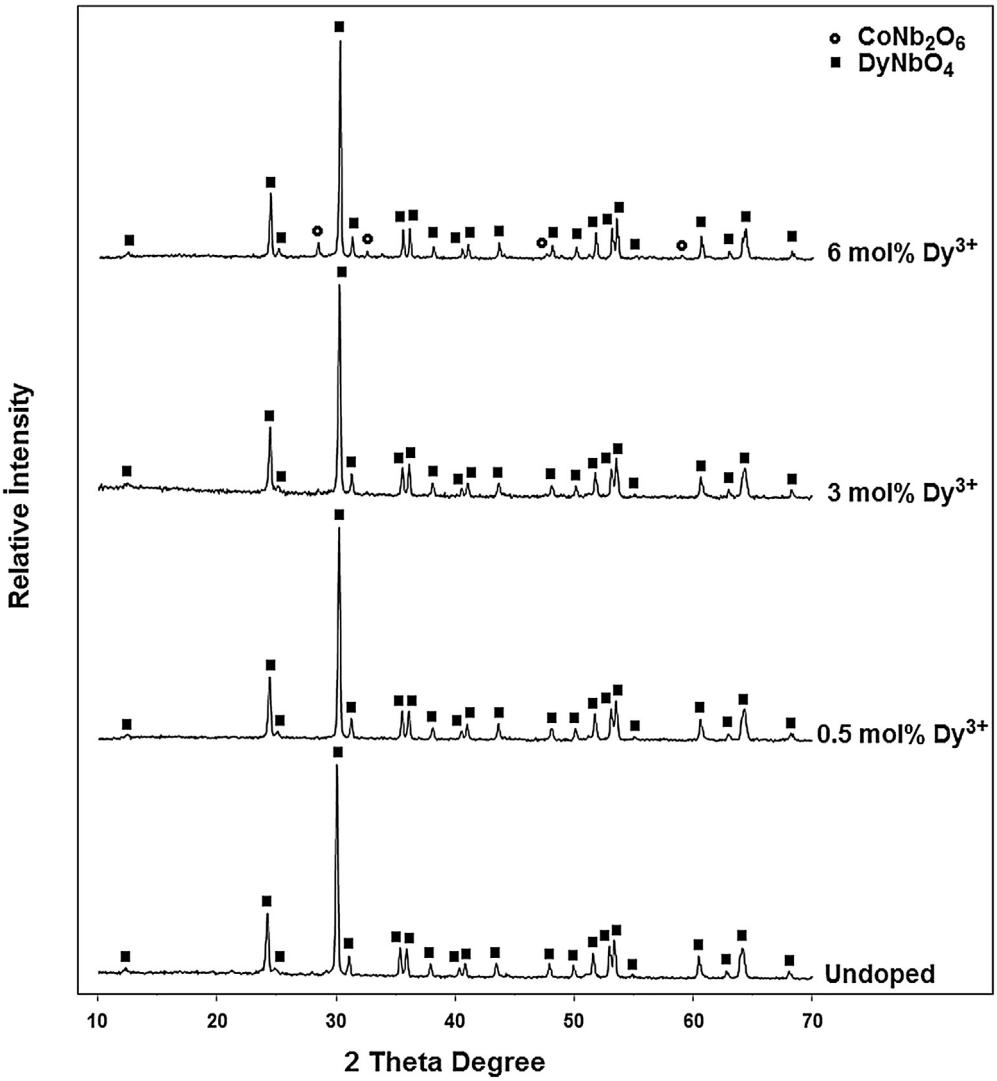

Fig. 1. X-ray diffraction patterns of undoped and Dy^{3+} doped $CoNb_2O_6$ structures.

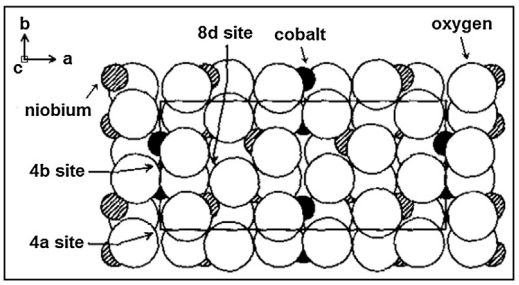

Fig. 2. Representation of $CoNb_2O_6$ columbite crystal structure projected along the c axis.

Fig. 5(a and b). In EDS analysis, small grains indicated the Dy^{3+} doped $CoNb_2O_6$ phase (point 1 in Fig. 5c). Elongated and large grains showed $DyNbO_4$ minor phase (point 2 in Fig. 5d). EDS analysis revealed that the elemental (identical with theoretical) compositions of Dy^{3+} doped $CoNb_2O_6$ grains (point 1) and $DyNbO_4$ large grains (point 2) were in agreement with the XRD results.

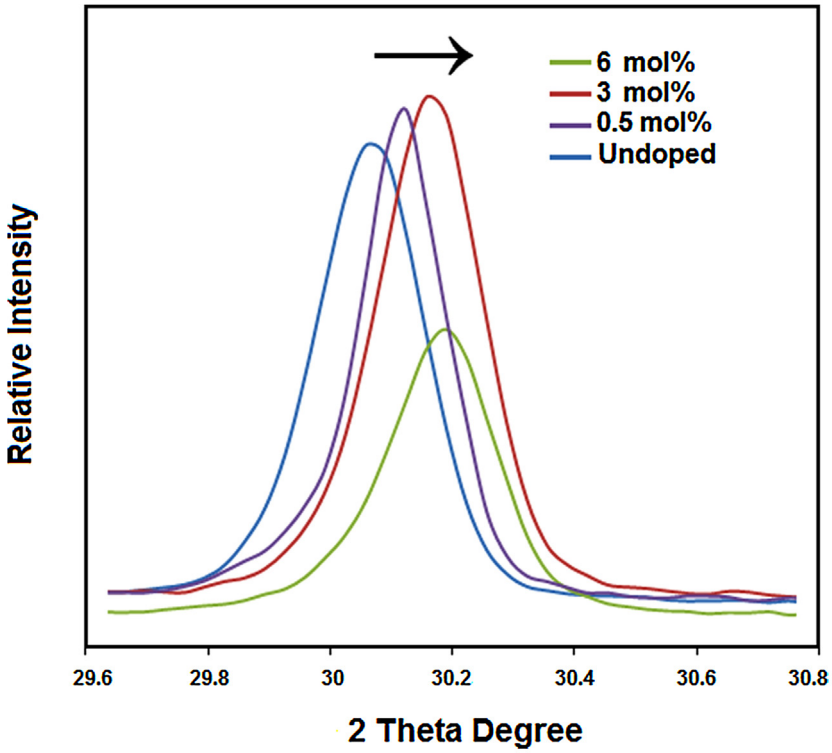

Fig. 3. Peak shifts (311) to higher two theta angles by increasing doping concentration.

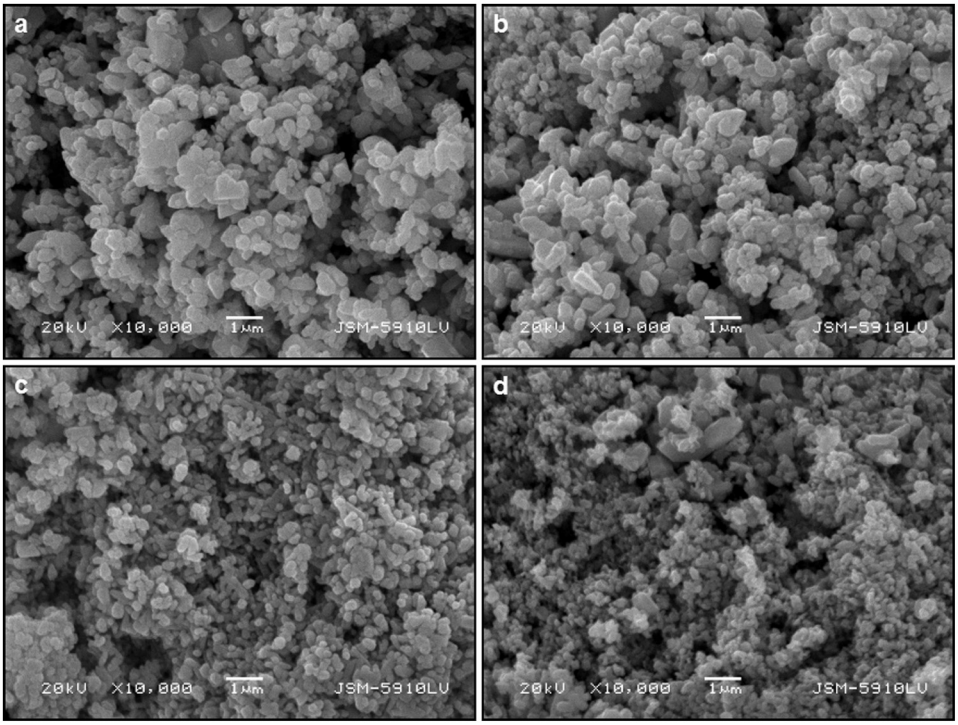

Fig. 4. SEM micrographs at 10.000× magnification of (a) undoped (b) 0.5, (c) 3, (d) 6 mol% Dy^{3+} doped $CoNb_2O_6$ structures.

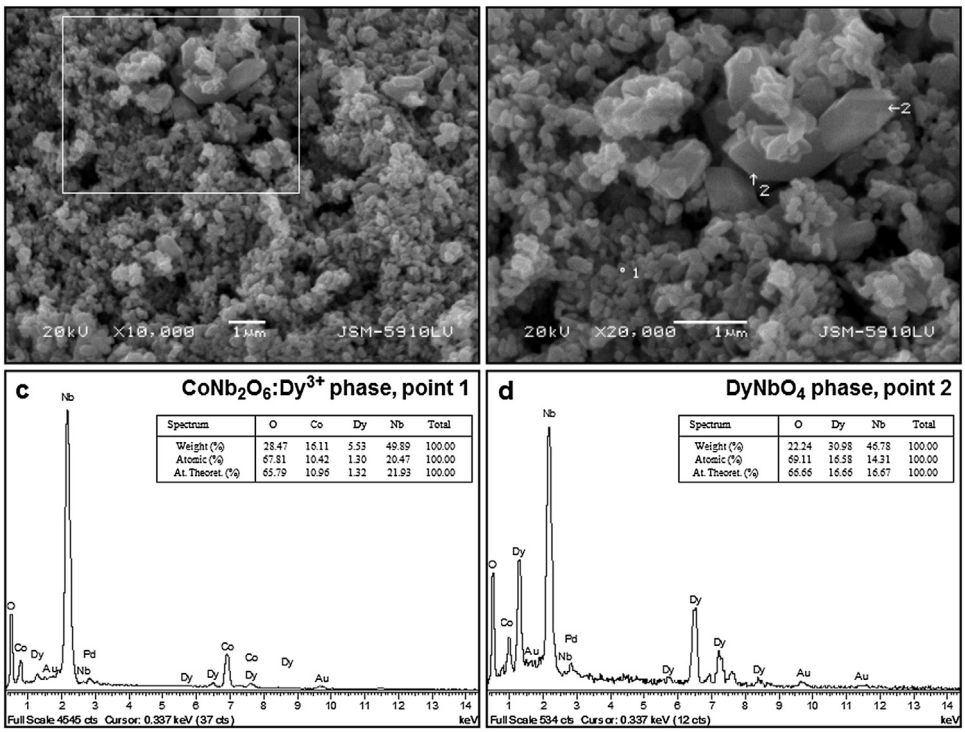

Fig. 5. SEM micrographs of 6 mol% Dy^{3+} doped sample at magnifications (a) low (10.000×), (b) high (20.000×) and EDS spectra (c) $CoNb_2O_6$:Dy^{3+} phase (point 1), (d) $DyNbO_4$ phase (point 2).

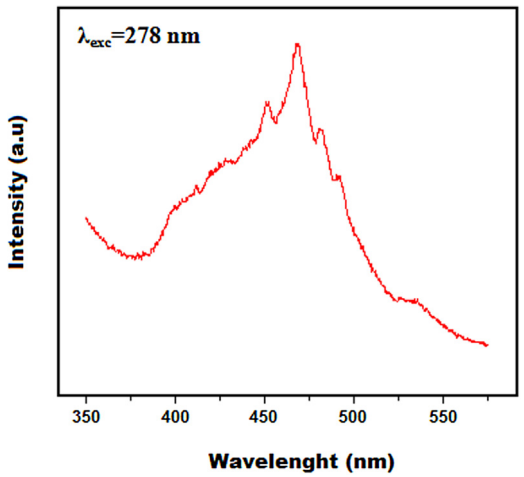

Fig. 6. Emission spectrum of $CoNb_2O_6$ host at λ_{ex} = 278 nm.

From the XRD and SEM-EDS results, the charge compensation of Dy^{3+} doped $CoNb_2O_6$ structure may be interpreted that changing charge balance in the lattice could be mostly based on lattice shrinking and small amount of minor phase formation above 3 mol%.

3.2. Optical characterization

Fig. 6 shows UV–vis emission spectra of undoped $CoNb_2O_6$ host which has given below. Excitation of undoped powder at 278 nm resulted in blue host luminescence at about 460 nm which ascribed to self-trapped exciton recombination [27]. Fig. 7 shows the excitation spectra of $CoNb_2O_6$:xDy^{3+} (x = 0.5, 3 and 6 mol%) phosphors with emission monitored at 579.2 nm. The excitation spectra in the 340–440 nm range belong to the transitions between the ground level $^6H_{13/2}$ and the excited levels $^4M_{15/2}$, $^4I_{11/2}$, $^4I_{13/2}$ and $^4G_{11/2}$, respectively. The assignments of the different excitation bands were identified on

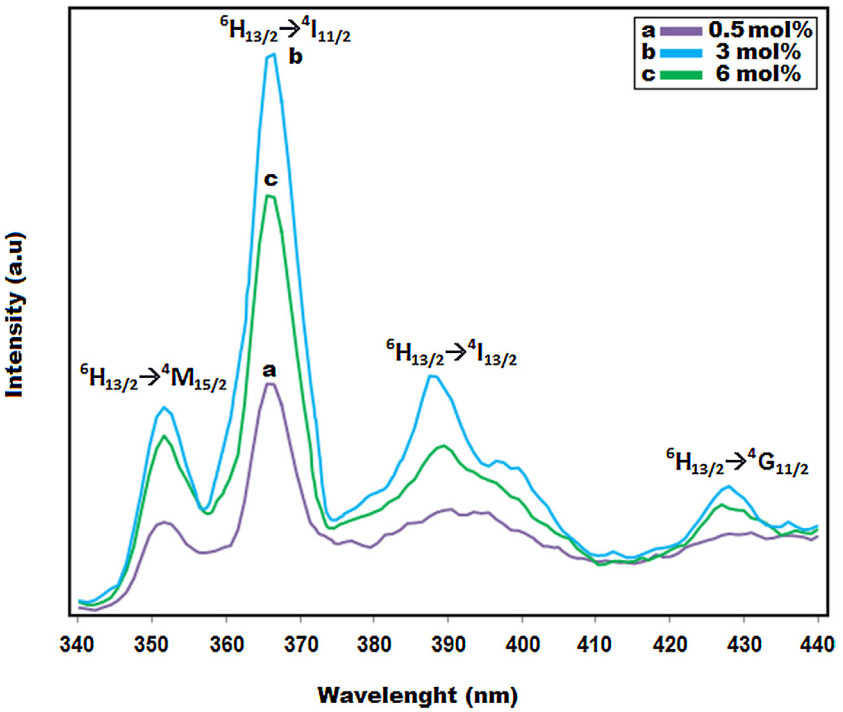

Fig. 7. Excitation spectra of $CoNb_2O_6$:Dy^{3+} phosphors monitored at 579.2 nm.

Table 1
CIE color coordinates, CCT data and Y/B ratios of $CoNb_2O_6$ phosphors at different Dy^{3+} concentrations and excited at λ_{ex} = 365.9 nm.

Dy^{3+} concentration (%)	Y/B	CIE coordinates		CCT
		x	*y*	
0.5	2.76	0.392	0.408	3924
3	3.96	0.419	0.428	3502
6	3.63	0.412	0.424	3608

the basis of Dieke's energy level diagram [28]. The excitation spectra contained four excitation bands which were observed at $^6H_{13/2} \rightarrow {}^4M_{15/2}$ (353.6 nm), $^6H_{13/2} \rightarrow {}^4I_{11/2}$ (365.9 nm), $^6H_{13/2} \rightarrow {}^4I_{13/2}$ (387.6 nm) and $^6H_{13/2} \rightarrow {}^4G_{11/2}$ (426.2 nm) transitions. Among these excitation bands, wavelength of 365.9 nm was chosen to carry out the photoluminescence properties of $CoNb_2O_6$:Dy^{3+}. Fig. 8 shows the emission spectra of $CoNb_2O_6$:xDy^{3+} (0.5, 3 and 6 mol%) samples under the excitation of 365.9 nm. The $CoNb_2O_6$:Dy^{3+} phosphors exhibited two emission bands at 484.5 nm (blue region) and 579.2 nm (yellow region). Blue and yellow regions are the characteristic emissions of Dy^{3+} attributed to the $^4F_{9/2} \rightarrow {}^6H_{15/2}$ and $^4F_{9/2} \rightarrow {}^6H_{13/2}$ transitions respectively. As seen from Table 1, high yellow/blue (Y/B) ratio indicated the presence of higher degree of interaction between dysprosium and oxygen ions [29]. This case may be explained by the incorporation of Dy^{3+} into octahedral (*4a,4b,8d*) sites in columbite structure which led to increase in the covalency. On the other hand, emission intensity increased by increasing of Dy^{3+} concentration, up to 3 mol% and then decreased due to concentration quenching effect that may be attributed to covalency which depends on the critical distance of Dy^{3+} ions and structural distortion.

The chromaticity coordinates (*x*,*y*) of $CoNb_2O_6$:Dy^{3+} phosphors with different doping concentrations excitation under 365.9 nm were listed in Table 1 which are declared by The Commission Internationale de l'Eclairage (CIE). The chromaticity coordinates of the $CoNb_2O_6$:Dy^{3+} phosphor were determined based on their corresponding PL spectra for different concentrations on the CIE chromaticity diagram. Fig. 9 shows the chromaticity coordinates of all $CoNb_2O_6$:Dy^{3+} phosphors located in the white region. For 3 mol% Dy^{3+} doped phosphor, chromaticity coordinates were estimated as (0.419, 0.428).

The light quality of a source is evaluated through the correlated color temperature (CCT) values which demonstrates the temperature of the closest Plankian black-body radiator to the operating point on the chromaticity diagram. The CCT values were calculated by using McCamy empirical formula (5) and was expressed as where $n = (x - x_e)/(y - y_e)$ is the inverse slope line, and x_e = 0.332 and y_e = 0.186 [30].

$$CCT = -449n^3 + 3525n^2 - 6823n + 5520.33 \quad (5)$$

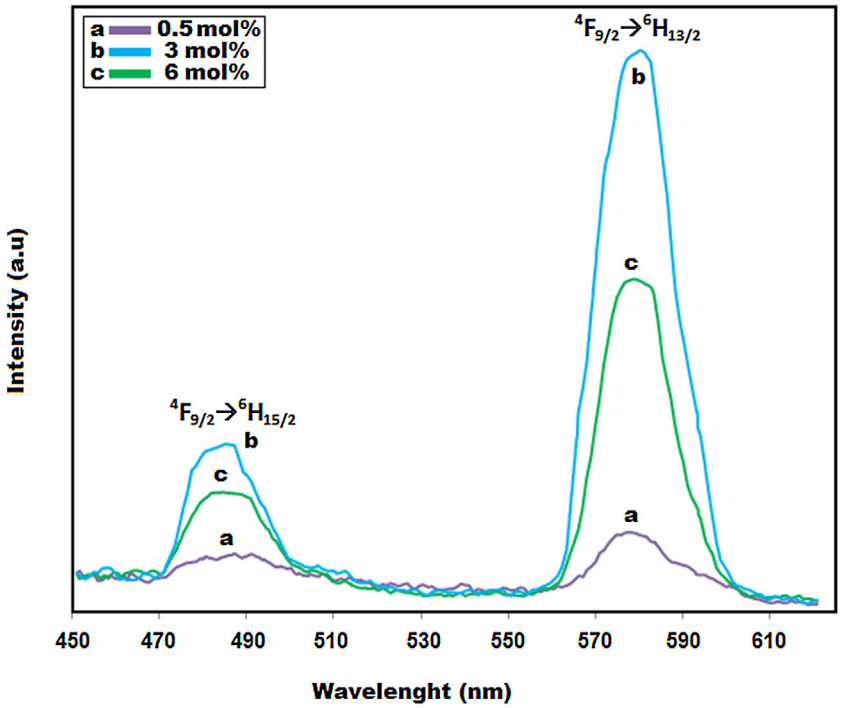

Fig. 8. Emission spectra of $CoNb_2O_6$:Dy^{3+} phosphors excited at 365.9 nm.

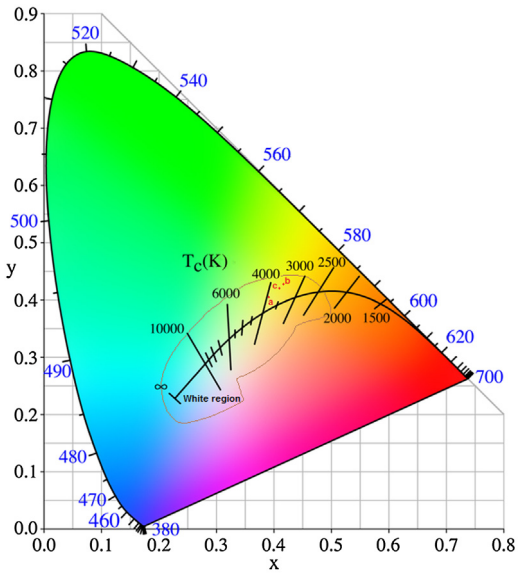

Fig. 9. CIE coordinates of the $CoNb_2O_6$:xDy^{3+} (x = a:0.5, b:3 and c:6 mol%) phosphors excited at 365.9 nm.

The CCT values at different concentrations were presented in Table 1. The CCT values for the $CoNb_2O_6$:Dy^{3+} phosphors were found between 3502 and 3924 K. It was found that the CCT value for 3 mol% was 3502 K. The CCT data of all samples have been estimated in white light region and color of light appear close to yellowish-green. Preferably, CCT values range from 3500 to 6500 K, but the range from 3000 to 7800 K is also acceptable in the literature. As seen in Table 1, the CCT values of all the phosphors were found to be lower than that of the standard white light luminescence. The present study indicates that the Dy^{3+} doped cobalt niobate phosphor are expected to be a promising candidate as emitting phosphor for sunrise/sunset white light emitting diodes.

4. Conclusion

Undoped, 0.5, 3 and 6 mol% Dy^{3+} doped $CoNb_2O_6$ crystalline powders were successfully synthesized by molten salt synthesis method at a relatively low temperature than that of the other traditional conventional methods. XRD analysis showed that undoped, 0.5 and 3 mol% Dy^{3+} doped powders exhibited single phase with orthorhombic structure. Photoluminescence of $CoNb_2O_6$:Dy^{3+} phosphors exhibited a blue emission at $^4F_{9/2} \rightarrow {}^6H_{15/2}$ (484.5 nm) transition and a yellow emission $^4F_{9/2} \rightarrow {}^6H_{13/2}$ (579.2 nm) transition. Emission intensity increased between 0.5 and 3 mol%, and then decreased due to concentration quenching effect. The calculated CCT data of all the phosphors were located in the white light region. Based on the observed results, it was concluded that the $CoNb_2O_6$:Dy^{3+} phosphor has potential for white LED applications.

References

[1] L.L. Shi, Y.L. Cheng, S. Qiang, J. Fluoresc. 21 (2011) 1461–1466.
[2] C.H. Yang, G.F. Yang, Y.X. Pan, Q.Y. Zhang, J. Fluoresc. 19 (2008) 105–109.
[3] K.N. Shinde, S.J. Dhoble, J. Fluoresc. 21 (2011) 2053.
[4] R.S. Ukare, V. Dubey, G.D. Zade, S.J. Dhoble, J. Fluoresc. 26 (2016) 791–806.
[5] H.J. Devi, R.S. Wairokpam, R.S. Loitongbam, J. Fluoresc. 26 (2016) 875–889.
[6] R. Shrivastava, J. Kaur, V. Dubey, J. Fluoresc. 26 (2016) 105–111.
[7] R. Coldea, D.A. Tennant, E.M. Wheeler, E. Wawrzynska, D. Prabhakaran, M. Telling, K. Habicht, P. Smeibidl, K. Kiefer, Science 327 (2010) 177.
[8] R.C. Pullar, J. Am. Ceram. Soc. 92 (2009) 563.
[9] Y.J. Hsiao, C.W. Liu, B.T. Dai, Y.H. Chang, J. Alloys Comp. 475 (2009) 698.
[10] J.H. Sturdivant, Zeitschrift Kristallogr. 75 (1930) 88–105.
[11] C.A. dos Santos, L.I. Zawislak, E.J. Kinast, V. Antonietti, B.M.J. da Cunha, Braz. J. Phys. 31 (2001) 616–631.
[12] A.J. Moulson, J.M. Herbert, Electroceramics: Materials, Properties, Appications, Chapman and Hall, New York, 1990.
[13] A.S. Bhalla, R. Guo, R. Roy, Mat. Res. Innovat. 1 (2000) 3–26.
[14] S. Kobayashi, S. Mitsuda, M. Ishikawa, K. Miyatani, K. Kohn, Phys. Rev. B: Condens. Matter 60 (1999) 3331.
[15] C. Balamurugan, A.R. Maheswari, D.W. Lee, Sens. Actuators B 205 (2014) 289–297.
[16] N. Vittayakorn, T. Tunkasiri, Phys. Scr. 129 (2007) 199–204.
[17] T.R. Shrout, A. Halliyal, Am. Ceram. Soc. Bull. 66 (1987) 704–711.
[18] S. Mitsuda, H. Okano, S. Kobayashi, K. Prokes, J. Magn. Magn. Mater. E 993 (2004) 272–276.
[19] R.C. Pullar, K. Okeneme, N. McN. Alford, J. Eur. Ceram. Soc. 23 (2003) 2479.
[20] V. Parvlescu, M. Ruwet, P. Grange, V.I. Parvlescu, Solid State Ionics 137 (1997) 101–103.
[21] N. Chaiyo, N. Vittayakorn, J. Ceram. Process. Res. 9 (2008) 381–384.
[22] I.S. Mulla, N. Natarajan, A.B. Gaikwad, V. Samuel, U.N. Guptha, V. Ravi, Mater. Lett. 61 (2007) 2127–2129.
[23] R. Ma, F. Cao, J. Wang, G. Zhu, G. Pang, Mater. Lett. 65 (2011) 2880–2882.
[24] K.H. Yoon, Y.S. Cho, D.H. Lee, D.H. Kang, J. Am. Ceram. Soc. 76 (1993) 1373–1376.
[25] K.H. Yoon, Y.S. Cho, D.H. Kang, J. Mater. Sci. 33 (1998) 2977–2984.
[26] M. Sato, Y.J. Hama, J. Solid State Chem. 118 (1995) 193–198.
[27] A.M. Srivastava, J.F. Ackerman, W.W. Beeers, J. Solid State Chem. 134 (1997) 187–191.
[28] G.H. Dieke, Spectra and Energy Levels of Rare Earth Ions in Crystals, Interscience Publishers, New York, 1968.
[29] N. Vijaya, K.U. Kumar, C.K. Jayasankar, Spectrochim. Acta Part A 113 (2013) 145–153.
[30] C.S. McCamy, Color Res. Appl. 17 (1992) 142–144.